

Photoionization of $\text{Na}(\text{NH}_3)_n$ and $\text{Na}(\text{H}_2\text{O})_n$ Clusters: A Step Towards the Liquid Phase?

I. V. Hertel, C. Hüglin, C. Nitsch, and C. P. Schulz

Freiburger Materialforschungszentrum der Albert-Ludwigs-Universität, W 7800 Freiburg, Germany
(Received 6 May 1991)

Ionization potentials (IP's) for $\text{Na}(\text{H}_2\text{O})_n$ and $\text{Na}(\text{NH}_3)_n$ are reported for the first time up to $n=20$. As expected, for $\text{Na}(\text{NH}_3)_n$ the IP decreases more or less monotonically with decreasing $(n+1)^{-1/3}$ to a limit consistent with the bulk value of 1.45 eV. In contrast, for $\text{Na}(\text{H}_2\text{O})_n$ we find the IP as a function of $(n+1)^{-1/3}$ to be constant at 3.17 eV for $n \geq 4$, close to the bulk value. For comparison we solve a one-electron Schrödinger equation in a dielectrically screened Coulomb potential. While agreement with the experiment is reasonable for small n , this one-center model fails for larger clusters, thus giving some first indication for the existence of two-center localized states in these microclusters.

PACS numbers: 61.90.+d, 33.80.Eh, 36.40.+d, 82.40.Dm

Solvated electrons have been studied for a long time in liquids of polar molecules, see, e.g., [1-4]. Recently, the observation of isolated negative water and ammonia clusters [5,6] and the progress in theoretical methods [7,8] have focused much renewed attention on this celebrated subject. The fascinating discussion about surface versus bulk states [7,9] and dynamical aspects of the solvation phenomenon [10] seems to have replaced earlier controversies on the nature of the solvation process. In ammonia, e.g., traditionally the "solvated" electron was observed in dilute solutions of alkali metals [1,2] and two competing models were used to describe the experimental observations: (a) the electron trapped around the cation embedded in the dielectric and (b) the cavity model in which the electron is separated from the cation and both are screened individually by the surrounding dielectric medium. Strong experimental evidence (see, e.g., Ref. [5]) favors the latter two-center localization model for the bulk phase, while for isolated atoms surrounded by a few solvent molecules we would expect the former picture to hold. Preparation of molecular clusters in supersonic beams allows us to study such aggregates as free species and thus to follow the building up of the liquid phase from its constituents. Recently, we were able to report first measurements of the photoionization threshold for small $\text{Na}(\text{H}_2\text{O})_n$ [11] and $\text{Na}(\text{NH}_3)_n$ clusters [12]. These data were in good agreement with the available *ab initio* calculations for small $\text{Na}(\text{H}_2\text{O})_n$; however, the maximum size observed was much too small to extrapolate any trend towards the bulk value and thus a comparison with models of the above type was not possible.

In the present work we report for the first time a measurement of the photoionization potential, IP, for solvated $\text{Na}(\text{H}_2\text{O})_n$ and $\text{Na}(\text{NH}_3)_n$ with n up to 20, and an upper bound for $\text{Na}(\text{NH}_3)_n$, $n \leq 35$, and we compare it with a one-center model calculation. This allows us to relate the measured binding energies of the electron to the bulk limit and to emphasize indications of two-center effects. We also present an illuminating comparison with electron affinities for the neutral solvent clusters for which comprehensive data are now available [6]. The present results thus offer intriguing new insights and provide

challenging material for rigorous quantum calculations attempting a unified treatment of the solvated electron and metal atom.

The experimental setup for determining the ionization potentials is essentially identical to that described previously [12]. The $\text{Na}(\text{H}_2\text{O})_n$ and $\text{Na}(\text{NH}_3)_n$ clusters are prepared in a "pickup" source where an effusive sodium beam is exposed to a pulsed supersonic beam of a mixture of H_2O and Ar (or neat NH_3 , respectively) in the high-pressure expansion zone. The thus created cluster beam passes through a 1.5-mm-diam skimmer and reaches the ionization zone 15 cm downstream. We use either an excimer-pumped dye laser or a frequency-doubled dye laser pumped by the second harmonics of a Nd-doped yttrium-aluminum-garnet laser to ionize the cluster beam. Mass separation of the ionized products occurs in a standard linear time-of-flight spectrometer (ion energy 390 eV, field-free flight path 55 cm). Careful analysis of the observed signals as a function of laser power ensures that we detect the photoionization thresholds of the molecular clusters in the linear one-photon regime.

For the $\text{Na}(\text{NH}_3)_n$ system photoionization thresholds and structure of the mass spectra show interesting peculiarities, details of which will be presented in a forthcoming publication. The first solvation shell at $n=4$ reported for the solvated sodium cation [13] is only seen weakly for the neutral. In contrast, the present work for $\text{Na}(\text{H}_2\text{O})_n$ presents a much more pronounced situation. Figure 1 shows the mass spectra for $n \geq 4$ at five different photon energies $h\nu < \text{IP}[\text{Na}(\text{NH}_3)_3]$. The signals were obtained for otherwise identical conditions and have been normalized to the laser intensity. Surprisingly, these mass spectra show a dramatic drop of the ion intensity, almost simultaneously for $n=4$ to $n=23$, in between $h\nu=3.147$ and 3.108 eV. We therefore determine the photoionization potential of $\text{Na}(\text{H}_2\text{O})_4$ to $\text{Na}(\text{H}_2\text{O})_{20}$ to be $\text{IP}=3.17(5)$ eV. In Fig. 2 our ionization potentials for $\text{Na}(\text{H}_2\text{O})_n$ and $\text{Na}(\text{NH}_3)_n$ are shown as a function of $(n+1)^{-1/3}$, the latter being roughly inversely proportional to the cluster radius R_c including the Na^+ core. For comparison we have also reproduced the essentials of the measured vertical electron affinities of $(\text{H}_2\text{O})_n$ and

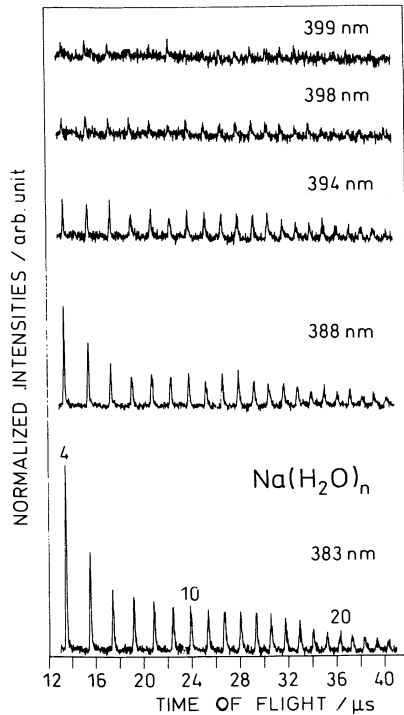


FIG. 1. Time-of-flight mass spectra for $\text{Na}(\text{H}_2\text{O})_n$ ($n \geq 4$) at five different photon energies: 399 nm (3.108 eV), 398 nm (3.115 eV), 394 nm (3.147 eV), 388 nm (3.196 eV), 383 nm (3.237 eV).

$(\text{NH}_3)_n$ reported by Lee *et al.* [6] as well as the (bulk) ionization potential for dilute solutions of Na in ammonia [2] (1.45 eV) and for electrons solvated in water (3.2 eV), as derived from photoconduction threshold and width of the conduction band [6].

Several remarkable features are displayed in Fig. 2. For Na in water, the IP decreases rapidly with cluster size until the first solvation shell at $n=4$ is filled (by a total of nearly 2 eV with respect to the isolated Na atom) and, as pointed out above, stays constant for $n \geq 4$. One possibility for explaining this surprising behavior would be to assume that the solvated Na is completely screened by the first solvation shell. More likely, however, the break marks the onset of a new type of state, possibly the two-center localization mentioned above. This finding has to be contrasted with the electron affinities (EA) of the negative clusters [5] which show almost perfect agreement with the dielectric screening theory of Barnett *et al.* [7] which predicts a linear increase of the EA with [14] $n^{-1/3}$, the experimentally observed slope being almost identical to the predicted value $(1+1/\epsilon_{\text{opt}} - 2/\epsilon_{\text{stat}})/2R_{\text{WS}}$. Here ϵ_{opt} and ϵ_{stat} are the optical and static dielectric constants and R_{WS} the Wigner-Seitz radius of the solvent (for H_2O $\epsilon_{\text{opt}}=1.76$, $\epsilon_{\text{stat}} \sim 78$, $R_{\text{WS}} \sim 3.8a_0$).

For ammonia as a solvent we do not see such a drastic break in the experimental data. We observe again an

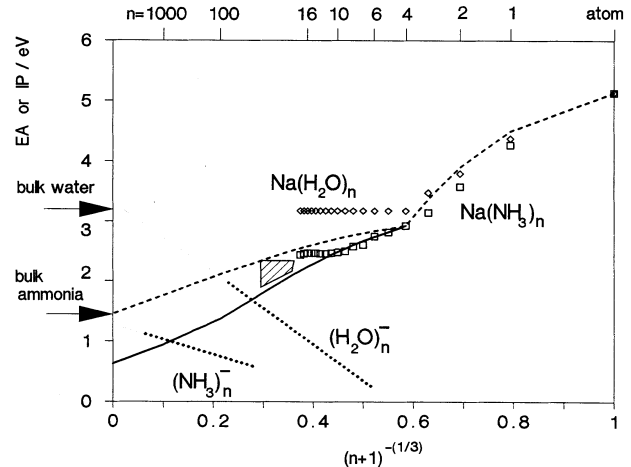


FIG. 2. Experimental ionization potentials of $\text{Na}(\text{H}_2\text{O})_n$ (diamonds) and $\text{Na}(\text{NH}_3)_n$ (squares) vs $(n+1)^{-1/3}$, the shaded area giving an upper bound for $20 < n < 35$. Experimental errors correspond to the size of the symbols. The dashed line represents the calculated IP's using the model potential for dielectric screening; the solid line for $n \geq 5$ includes the self-consistent-field screening potential (see text). For comparison measured electron affinities [7] for $(\text{H}_2\text{O})_n^-$ and $(\text{NH}_3)_n^-$ (dotted lines) are also shown.

(even stronger) drop of the IP between the atom and closure of the first solvation shell at $\sim \text{Na}(\text{NH}_3)_4$. However, with the addition of further NH_3 the IP drops further. Upon closer inspection of the results one does, nevertheless, recognize a more or less flat region between $n=10$ and $n=16$ which might have a similar origin to that observed in $\text{Na}(\text{H}_2\text{O})_n$ for $n \geq 4$. Eventually the ionization potential has to decrease again in order to reach the bulk value. Two further experimental observations are significant in this context: We have not seen cluster ions with 532 nm, providing an upper limit of the IP ≤ 2.33 eV for $20 < n < 50$, and we have measured photoelectron energies from clusters of (yet undetermined) larger size indicating IP's of at least down to 1.9 eV [C. Nitsch *et al.* (to be published)]. Thus, our observations are consistent with a straight-line extrapolation of the IP between $n=16$ and ∞ as a function of $(n+1)^{-1/3}$ leading to the bulk value of 1.45 eV [2]. This implies three different regions for the decrease of the IP in $\text{Na}(\text{NH}_3)_n$ in contrast to two regions for $\text{Na}(\text{H}_2\text{O})_n$. For comparison, the electron affinities of $(\text{NH}_3)_n^-$, even though they too extrapolate very well and linearly with [14] $n^{-1/3}$, exhibit a slope which is not consistent with the simple dielectric screening prediction. The latter should be almost identical to the one for the H_2O case (only $\epsilon_{\text{stat}}=25$ is different for NH_3). In summary, $(\text{H}_2\text{O})_n^-$ behaves well with respect to the dielectric screening model, while $(\text{NH}_3)_n^-$ does not. In contrast, the one-center screening model for the solvated neutral Na atom appears to hold only up to $n \leq 4$ with H_2O molecules while for NH_3 the screening

increases further at least up to $n = 10$.

To quantify the last statement, and lacking serious theoretical data such as, e.g., the quantum path-integral method applied for the negative ions [7], we resort to a simple one-electron one-center calculation, following the more conventional wisdom about solvated atoms. This should allow us to pinpoint departures from the one-center model expected to hold for small n towards two-center states expected for large n . We solve the one-electron Schrödinger equation for a spherical potential originating from the Na^+ core screened by its dielectric environment, essentially in the spirit of previous work [15]. We use a model potential with four different regions of electron distance from the Na^+ nucleus: For small $0 \leq r \leq R_1$ we take $V_1(r) = V_c(r) + C_1$, $V_c(r)$ being Aymar's [16] well-established Na^+ ion core which perfectly reproduces the $\text{Na}(3s)$ ground-state energy as well as a number of excited states. For R_1 we chose, somewhat arbitrarily but consistent with similar earlier assumptions, the sum of the ionic Na^+ core radius and the van der Waals radius for N or O, respectively. This region is followed by the first solvation shell, $R_1 \leq r \leq R_2$, the so-called *monomer* which we take to be Na^+ surrounded by four solvent molecules (for ammonia $R_1 = 4.66a_0$ and $R_2 = 7.27a_0$). There we assume the potential to be screened as $V_1(r) + q_{\text{eff}}n_{\text{eff}}/r + C_2$, with $n_{\text{eff}} = n$ for $n \leq 4$ and $n_{\text{eff}} = 4$ for $n \geq 4$. The effective screening charge q_{eff} is treated as a fit parameter and adjusted in such a manner that the calculation reproduces the experimental value for the IP of Na surrounded by four solvent molecules. The radius of the *monomer* R_2 is assumed to be $R_1 + R_d + R_H$, with R_d the bond length of the solvent molecule projected onto its symmetry axis and R_H the van der Waals radius of the H atom. From the *monomer* to the cluster radius, $R_2 \leq r \leq R_c = [R_2^3 + (n-4)R_{\text{WS}}^3]^{1/3}$, we use a screened Coulomb potential $V_3(r) = -1/\epsilon_{\text{opt}}r + C_3$. Finally, outside the cluster $R_c \leq r$ we use $V_4(r) = -1/r$. The constants C_1 , C_2 , and C_3 are adjusted so that the potential is continuous. The radial Schrödinger equation is solved by the Numerov algorithm to obtain binding energy $E = -\text{IP}$ and radial wave function $\psi(r)$; at $r = 5a_0$ the logarithmic derivatives of $u(r) = \psi(r)/r$ are matched for integration in and out from infinity and $r = 0$, respectively. For $n = 0$, this reproduces the correct IP = 5.14 eV of the atom. As an example, Fig. 3 shows the model potential for $\text{Na}(\text{NH}_3)_{16}$ together with $u(r)$. We see that the electron extends over a rather large range of the cluster.

The resulting IP's for the $\text{Na}(\text{NH}_3)_n$ case are displayed along with our experimental data in Fig. 2 (dashed line). More consequently, we have to introduce additional screening outside the monomer by allowing the electron itself to influence the orientation of the dielectric medium. This adds, as first discussed by Jortner [17], a screening term $\beta \int [1 - q(r)] r^{-2} dr$ with $q(r) = 4\pi \int u(r)^2 dr$ and $\beta = (1/\epsilon_{\text{opt}} - 1/\epsilon_{\text{stat}})$ to the potential

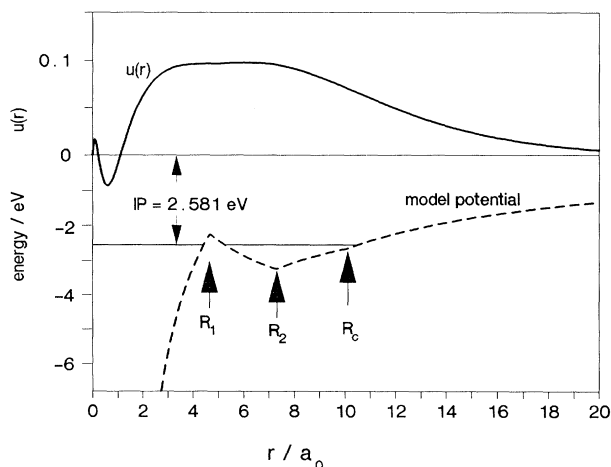


FIG. 3. Model potential used for $\text{Na}(\text{NH}_3)_{16}$ and radial part $u(r) = \psi(r)/r$ of the one-electron wave function $\psi(r)$ with Na^+ at the origin.

[in our case to $V_3(r)$]. Thus, $u(r)$ has to be determined in a self-consistent manner. We have applied this model in the spirit of similar calculations for the negative clusters [8] to derive IP's for $n \geq 5$. The results are also displayed in Fig. 2 (solid line). Considering that only one fitting parameter, the IP of $\text{Na}(\text{NH}_3)_4$, was used, the agreement between measurement and model calculation is very nice up to about ten, beyond which a clear departure results. In particular, the bulk value cannot be reproduced. We consider this observation to demonstrate the failure of the one-center model for larger n , giving evidence for the formation of two-center states. The discrepancy begins at about the same $n \sim 10$ where the IP tends to flatten out, as remarked above. Repeating the one-center calculation for $\text{Na}(\text{H}_2\text{O})_n$, we find it impossible to obtain any explanation for the measured IP's or even a resemblance of the experimentally found trend for $n > 4$. Since the parameters to be used are quite similar to those for ammonia, one-center dielectric screening always predicts a significant and nearly linear decrease of the IP's with decreasing $(n+1)^{-1/3}$. One would have to make rather artificial assumptions to reconcile the experimental observations with such a model. Again, we make two-center localization responsible for the remarkable behavior observed experimentally. It may be noted at this point that experimental evidence for ion-pair formation has also been seen in strontium cations solvated in ammonia clusters [18].

In conclusion, we see clear evidence of the departure from localized one-center states and for the formation of two-center states in $\text{Na}(\text{H}_2\text{O})_n$ for $n > 4$ beyond which the IP remains constant, supposedly up to the bulk limit. A similar, although less clear, trend is seen in $\text{Na}(\text{NH}_3)_n$ for $n > 10$ where the IP appears to flatten out up to at least $n = 16$. For still larger n the IP will again decrease.

This third, large- n region might indicate again a new type of state. Jortner [19] proposes that the flat regions are connected with the formation of two-center Na^+ -surface-electron states, while for larger clusters pairs of cation and interior electron states might be formed. The different behavior of ammonia and water as a solvent would then be closely reminiscent of the different stability of the surface excess electron states versus bulk electron states found for negative water and ammonia clusters [7,9]. We note in passing that we can derive from Fig. 2 an approximate empirical relation $\text{IP} - \text{EA} = 5.9n^{-1/3}$ between the measured ionization potentials of the solvated atom if extrapolated to large n and the electron affinities [6] of the neutral solvent clusters, for both H_2O and NH_3 . Comparing with the energy e^2/R_p needed to separate an ion pair, a critical electron-ion distance slightly larger than the cluster radius $R_p \sim 1.3R_{\text{WS}}n^{1/3}$ would account for that difference. This may be seen as additional support for the two-center-state explanation. Of course, such speculations will have to be borne out in rigorous quantum calculation. A unified theoretical treatment of these phenomena would thus be highly desirable and can now be met with sufficiently crucial experimental testing material.

We would like to thank J. Jortner very much for an extremely stimulating correspondence on the subject of the different two-center states. Financial support by the Deutsche Forschungsgemeinschaft through Sonderforschungsbereich No. 276 is gratefully acknowledged.

[1] W. Weyl, Ann. Phys. (Leipzig) **197**, 601 (1864); note that in the literature the year of this publication is consistently quoted incorrectly as 1863.

[2] J. Häsing, Ann. Phys. 5. Folge **37**, 509 (1940).

- [3] E. J. Hart and J. W. Boag, J. Am. Chem. Soc. **84**, 4090 (1962).
- [4] J. C. Thompson, *Electrons in Liquid Ammonia* (Oxford Univ. Press, Oxford, 1976).
- [5] H. Haberland, C. Ludewigt, H. G. Schindler, and D. R. Worsnop, Surf. Sci. **156**, 157 (1985).
- [6] G. H. Lee, S. T. Arnold, J. G. Eaton, H. W. Sarkas, K. H. Bowen, C. Ludewigt, and H. Haberland, Z. Phys. D (to be published).
- [7] R. N. Barnett, U. Landman, C. L. Cleveland, and J. Jortner, Chem. Phys. Lett. **145**, 382 (1988); **148**, 249 (1988).
- [8] P. Stampfli and K. H. Bennemann, Phys. Rev. Lett. **58**, 2635 (1987).
- [9] R. N. Barnett, U. Landman, C. L. Cleveland, and J. Jortner, Phys. Rev. Lett. **59**, 811 (1987).
- [10] R. N. Barnett, U. Landman, and A. Nitzan, Phys. Rev. Lett. **62**, 106 (1988).
- [11] C. P. Schulz, R. Haugstätter, H.-U. Tittes, and I. V. Hertel, Phys. Rev. Lett. **57**, 1703 (1986); Z. Phys. D **10**, 279 (1988).
- [12] C. P. Schulz, A. Gerber, C. Nitsch, and I. V. Hertel, Z. Phys. D **20**, 65 (1991).
- [13] T. D. Märk and A. W. Castleman, Jr., Adv. At. Mol. Phys. **30**, 65 (1985).
- [14] Note that for the large clusters in this plot n and $n+1$ are almost identical.
- [15] See, e.g., D. A. Copeland, N. R. Kestner, and J. Jortner, Chem. Phys. **53**, 1189 (1970); W. E. Blumberg and T. P. Das, J. Chem. Phys. **30**, 251 (1959).
- [16] M. Aymar (private communication):
- $$rV_c(r) = -10\exp(-7.88747r) + 23.54102r\exp(-2.69155r) + 1.$$
- [17] J. Jortner, J. Chem. Phys. **34**, 678 (1961).
- [18] M. H. Shen and J. M. Farrar, J. Phys. Chem. **93**, 4386 (1989).
- [19] J. Jortner (private communication).